ON THE COMPUTATION OF PHASE AND ENERGY GAIN FOR A THIN-LENS RF GAP USING A GENERAL FIELD PROFILE*

C.K. Allen, Oak Ridge National Laboratory, Oak Ridge, Tennessee 37831 USA

Abstract

The thin-lens representation for an RF accelerating gap has been well developed and is documented by Lapostolle [1], Weiss [2], Wangler [3], and others [4], [5]. These models assume that the axial electric field is both centered and symmetric so it has a cosine expansion. Presented here is a model that considers general axial fields. Both the cosine and sine transit time factors are required plus their Hilbert transforms. The combination yields a complex Hamiltonian rotating in the complex plane with the synchronous phase. The phase and energy gains are computed in the pre-gap and post-gap regions then aligned with asymptotic values of wave number. Derivations are outlined, examples are shown, and simulations presented.

BACKGROUND

Thin Lens

Let an RF accelerating gap be centered at axial position $z = 0$. In the thin-lens model particle energy W is constant upstream and downstream but experiences an impulsive energy gain ΔW at $z = 0$. Hamiltonian dynamics require that particle phase ϕ must also experience an impulse $\Delta\phi$ at $z = 0$. The objective is to determine the final phase and energy (ϕ_0^+, W^+) given an arbitrary longitudinal electric field profile $\mathfrak{E}_z(z,t)$ and initial coordinates (ϕ_0^-, W^-).

Assuming that the gap axial field $\mathfrak{E}_z$ is harmonic, the spatial and time dependence can be separated as

$$\mathfrak{E}_z(z,t) = E_z(z)\cos\phi(t)\,, \tag{1}$$

where $E_z(\cdot)$ is the profile of the longitudinal electric field component. The RF phase is given by $\phi(t) = \omega t + \phi_0$ where $\omega = 2\pi f$ is the RF angular frequency and ϕ_0 is the phase at time $t = 0$ when the particle is at $z = 0$. If $z = z(t)$ is the particle position at time t then the phase $\phi(z)$ seen *by the particle* can be expressed

$$\phi(z) = 2\pi f \int_0^z \frac{1}{\beta(s)c}\,ds + \phi_0 = \int_0^z k(s)\,ds + \phi_0\,, \qquad \approx \bar{k}z + \phi_0, \tag{2}$$

where $\beta(z)$ is the normalized particle velocity, c is the speed of light, $k(z) = 2\pi/\beta(z)\lambda_{RF}$ is the particle wave number, and λ_{RF} is the RF wavelength. The second line assumes the particle velocity is constant $\bar{\beta}$ producing an averaged wave number $\bar{k}$, accurate when $\Delta W \ll W^-$.

Laplace Transform and Hilbert Transform

The two-sided Laplace transform $\mathcal{L}_2$ of real function f is defined [6]

$$\mathcal{L}_2[f(z)](\sigma) \triangleq AC \int_{-\infty}^{+\infty} f(z)e^{-\sigma z}\,dz\,, \tag{3}$$

where AC indicates analytic continuation and $\sigma = \phi + ik \in \mathbb{C}$ is the complex transform variable. Define $\mathcal{E}_z(\sigma) \triangleq \mathcal{L}_2[E_z(z)](\sigma)$. From (3) and the Euler identity

$$\mathcal{E}_z(ik) = V_0 T_z(k) - iV_0 S_z(k)\,, \tag{4}$$

where $V_0 \triangleq \int E_z dz$ is the potential across the gap, and

$$T_z(k) \triangleq \frac{1}{V_0}\int_{-\infty}^{+\infty} E_z(z)\cos kz\,dz\,,$$
$$S_z(k) \triangleq \frac{1}{V_0}\int_{-\infty}^{+\infty} E_z(z)\sin kz\,dz\,, \tag{5}$$

are the Fourier transform components of $E_z(\cdot)$ [7][8] known as *transit time factors* in beam physics [4].

The Hilbert transform $\mathcal{H}$ of real function f is [9]

$$\mathcal{H}[f](z) \triangleq PV\frac{1}{\pi}\int_{-\infty}^{+\infty}\frac{f(\zeta)}{z-\zeta}d\zeta = \frac{1}{\pi z} * f(z)\,, \tag{6}$$

where PV is the Cauchy principle value. The Hilbert transform is the convolution of $f(z)$ with the kernel $1/\pi z$. By the convolution property of Laplace transform $\mathcal{L}_2$ [6]

$$\mathcal{H}[\mathcal{E}_z(ik)] = \frac{1}{i\pi k} * \mathcal{E}_z(ik) = i\mathcal{L}_2[\mathrm{sgn}(z)E_z(z)]\,, \tag{7}$$

where $\mathrm{sgn}(z)$ (signum) is the inverse Laplace transform of $1/2\sigma$. Now define the *quadrature transform* $\mathcal{E}_q$ as

$$\mathcal{E}_q(\sigma) \triangleq \mathcal{L}_2[\mathrm{sgn}(z)E_z(z)](\sigma)\,. \tag{8}$$

The *quadrature transit-time factors* T_q and S_q are defined

$$T_q(k) \triangleq \frac{1}{V_0}\int_{-\infty}^{+\infty} \mathrm{sgn}(z)E_z(z)\cos kz\,dz\,,$$
$$S_q(k) \triangleq \frac{1}{V_0}\int_{-\infty}^{+\infty} \mathrm{sgn}(z)E_z(z)\sin kz\,dz\,, \tag{9}$$

so that

* This manuscript has been authored by UT-Battelle, LLC under Contract No. DE-AC05-00OR22725 with the U.S. Department of Energy. The United States Government retains and the publisher, by accepting the article for publication, acknowledges that the United States Government retains a non-exclusive, paid-up, irrevocable, worldwide license to publish or reproduce the published form of this manuscript, or allow others to do so, for United States Government purposes. The Department of Energy will provide public access to these results of federally sponsored research in accordance with the DOE Public Access Plan (http://energy.gov/downloads/doe-public-access-plan).

Copyright © 2017 CC-BY-3.0 and by the respective authors

$$\mathcal{E}_q(ik) = V_0 T_q(k) - iV_0 S_q(k)\,. \qquad (10)$$

By linearity of $\mathcal{H}$, Eqs. (7), (8), and (9), note $T_q(k) = -\mathcal{H}[S_z(k)]$ and $S_q(k) = +\mathcal{H}[T_z(k)]$. In principle T_q and S_q can be computed from T_z and S_z [10]. However, it may be more practical to compute them directly from Eqs. (9).

Pre- and Post- Envelopes

Define *pre- and post-envelopes* $\mathcal{E}^-$ and $\mathcal{E}^+$ as [9][11]

$$\begin{aligned} \mathcal{E}^- &\triangleq \frac{1}{2}(\mathcal{E}_z + i\mathcal{H}[\mathcal{E}_z]) = \frac{1}{2}(\mathcal{E}_z - \mathcal{E}_q)\,, \\ \mathcal{E}^+ &\triangleq \frac{1}{2}(\mathcal{E}_z - i\mathcal{H}[\mathcal{E}_z]) = \frac{1}{2}(\mathcal{E}_z + \mathcal{E}_q)\,. \end{aligned} \qquad (11)$$

Notice $\mathcal{E}^-(ik)$ and $\mathcal{E}^+(ik)$ are the spectra for half-fields

$$\begin{aligned} E^-(z) &\triangleq \begin{cases} E_z(z) & \text{for} \quad z < 0\,, \\ 0 & \text{for} \quad z > 0\,, \end{cases} \\ E^+(z) &\triangleq \begin{cases} 0 & \text{for} \quad z < 0\,, \\ E_z(z) & \text{for} \quad z > 0\,, \end{cases} \end{aligned} \qquad (12)$$

That is, $\mathcal{E}^{\pm}(ik) = \mathcal{L}_2[E^{\pm}](ik)$. Using Eqs. (4), (10), (11)

$$\begin{aligned} \mathcal{E}^-(ik) &= \frac{V_0}{2}[T_z - T_q] - i\frac{V_0}{2}[S_z - S_q], \\ \mathcal{E}^+(ik) &= \frac{V_0}{2}[T_z + T_q] - i\frac{V_0}{2}[S_z + S_q], \end{aligned} \qquad (13)$$

where T_z, T_q, S_z, S_z are all evaluated at k.

Since the data for $\mathcal{E}^-$ and $\mathcal{E}^+$ exists only on the imaginary axis $\sigma = ik$, the derivatives must be performed there. Via the Cauchy-Riemann conditions [12]

$$\begin{aligned} \mathcal{E}^{-\prime}(ik) &= -\frac{V_0}{2}(S_z' - S_q') - i\frac{V_0}{2}(T_z' - T_q')\,, \\ \mathcal{E}^{+\prime}(ik) &= -\frac{V_0}{2}(S_z' + S_q') - i\frac{V_0}{2}(T_z' + T_q')\,. \end{aligned} \qquad (14)$$

Quantities $\mathcal{E}^-, \mathcal{E}^{-\prime}, \mathcal{E}^+$, and $\mathcal{E}^{+\prime}$ determine the dynamics.

DYNAMICS

Energy Gain

The energy gained $\Delta W(z)$ by a particle up to axis location z is the work done by $\mathfrak{E}_z$ up to position $z(t)$ [3]. Using the expansion (1) for $\mathfrak{E}_z$ and the approximation in (2) for particle phase produces

$$\Delta W(\bar{k}; z) = q \int_{-\infty}^{z} E_z(s) \cos(\bar{k}s + \phi_0)\, ds\,. \qquad (15)$$

where q is particle charge and $\bar{k}$ is a suitable average wave number. Pivoting off the initial energy W^- for $z < 0$ and final energy W^+ for $z > 0$ the above formula yields the following for particle energy $W(z)$ for all z:

$$W(z) = \begin{cases} W^- + \displaystyle\int_{-\infty}^{z} qE_z \cos(\bar{k}^- s + \phi_0)\, ds & z < 0 \\ W^+ - \displaystyle\int_{z}^{+\infty} qE_z \cos(\bar{k}^+ s + \phi_0)\, ds & z > 0 \end{cases} \qquad (16)$$

where $\bar{k}^-$ and $\bar{k}^+$ are the upstream and downstream average wave numbers, respectively. Denote by $\Delta W^-$the (upstream) energy gain for $z < 0$ and by ΔW^+ the (downstream) energy gain for $z > 0$. Then

$$\begin{aligned} \Delta W^-(\phi_0, \bar{k}^-) &= Re\, q e^{-i\phi_0} \mathcal{E}^-(i\bar{k}^-), \\ \Delta W^+(\phi_0, \bar{k}^+) &= Re\, q e^{-i\phi_0} \mathcal{E}^+(i\bar{k}^+), \end{aligned} \qquad (17)$$

Phase Jump

Computation of the phase jump $\Delta\phi$ is more involved. The thin-lens phase approximation $\tilde{\phi}(z)$ is

$$\tilde{\phi}(z) \triangleq \begin{cases} k^- z + \phi_0^- & \text{for} \quad z < 0\,, \\ k^+ z + \phi_0^+ & \text{for} \quad z > 0\,, \end{cases} \qquad (18)$$

where k^- and k^+ are the pre- and post-gap wave numbers (i.e., $k^{\pm} = \lim_{z \to \pm\infty} k(z)$), and ϕ_0^- and ϕ_0^+ are the (constant) phase values at $z = 0^-$ and 0^+. The desired phase jump $\Delta\phi$ is the quantity $\Delta\phi = \phi_0^+ - \phi_0^-$ which realigns the asymptotic expressions in Eqs. (18) on either side of $z = 0$. Now define

$$\begin{aligned} \Delta\phi_0^- &\triangleq \phi_0 - \phi_0^-\,, \\ \Delta\phi_0^+ &\triangleq \phi_0^+ - \phi_0\,, \end{aligned} \qquad (19)$$

so that $\Delta\phi = \Delta\phi_0^+ + \Delta\phi_0^-$.

A variational technique is used to approximate particle phase $\phi(z)$. Expand wave number k in energy W about the asymptotic values k^- and k^+. Since $W(z)$ is known by Eq. (16) a first variation for $k(z)$ is formed. Consider first the upstream region $z < 0$. Wave number k can be expressed in terms of energy W as

$$k(W) = k_{RF} \frac{W + mc^2}{(W^2 + 2mc^2 W)^{1/2}}\,, \qquad (20)$$

where m is particle mass and $k_{RF} \triangleq 2\pi/\lambda_{RF}$. Expanding about the initial energy W^- produces

$$k(z) \approx k(W^-) + \frac{dk(W^-)}{dW}[W(z) - W^-]\,. \qquad (21)$$

Note $k^- \triangleq k(W^-)$ and define

$$K^- \triangleq -\frac{dk(W^-)}{dW} = k_{RF} \frac{1}{mc^2} \frac{1}{\beta^{-3}\gamma^{-3}}\,, \qquad (22)$$

where β^- is the pre-gap normalized velocity, and γ^- is the pre-gap relativistic factor (K^- is defined positive). Substitute Eq. (16) into (21) then the result into (2) yields

$$\begin{aligned} \phi(z) &\approx \phi_0 + k^- z \\ &\quad - K^- \int_0^z \int_{-\infty}^{s_1} qE_z(s_2) \cos(\bar{k}^- s_2 + \phi_0)\, ds_2\, ds_1\,, \end{aligned} \qquad (23)$$

valid for $z < 0$. The asymptotic nature of $\tilde{\phi}$ requires $\phi(z) - \tilde{\phi}(z) \to 0$ as $z \to -\infty$. Using approximation (23), definitions (18), and $\Delta\phi_0^- = \phi_0 - \phi_0^-$ from (19)

ISBN 978-3-95450-182-3

Copyright © 2017 CC-BY-3.0 and by the respective authors

$$\Delta\phi_0^- \approx -K^- \int_{-\infty}^{0}\int_{-\infty}^{z} qE_z(s)\cos(\bar{k}s+\phi_0)\,ds\,dz\,, \\ = -K^- \int_{-\infty}^{0}\int_{s}^{0} qE_z(s)\cos(\bar{k}s+\phi_0)\,dz\,ds\,, \tag{24}$$

where the integration order was changed in the second line (note the domain $s < z < 0, -\infty < s < 0$). Carrying out the integration over z

$$\Delta\phi_0^- \approx Re\, qK^- e^{-i\phi_0} \int_{-\infty}^{+\infty} sE^-(s)\, e^{-i\bar{k}^- s} ds, \tag{25}$$

where the half-field E^- is substituted to extend the limits of integration. Using the Laplace derivative theorem [6]

$$\Delta\phi_0^- \approx Re\, qK^- e^{-i\phi_0}\{-\mathcal{E}^{-\prime}(\sigma)\}_{\sigma=i\bar{k}^-}\,, \tag{26}$$

where $\mathcal{E}^{-\prime}(\sigma) \triangleq d\mathcal{E}^-(\sigma)/d\sigma$, then evaluated at $\sigma = ik$.

The post-gap phase jump $\Delta\phi_0^+$ can be determined with an analogous procedure. The results for both regions are

$$\Delta\phi_0^-(\phi_0,\bar{k}^-) = Re - qK^- e^{-i\phi_0}\mathcal{E}^{-\prime}(i\bar{k}^-)\,, \\ \Delta\phi_0^+(\phi_0,\bar{k}^+) = Re - qK^+ e^{-i\phi_0}\mathcal{E}^{+\prime}(i\bar{k}^+)\,. \tag{27}$$

Eqs. (17) and (27) form the dynamics of the gap. They are coupled through the energy-momentum (i.e., wavenumber) relation (20), and definition (22).

Gap Offsets

By the shifting property of the Laplace transform any offset Δz_0 of the gap center from the axis origin can be represented as a multiplication of the spectrum $\mathcal{E}^-(ik)$ and $\mathcal{E}^+(ik)$ by $e^{-ik\Delta z_0}$ [6].

Hamiltonian Dynamics

Equations (17) and (27) suggest the following complex "Hamiltonians" $H^-, H^+ : \mathbb{C} \to \mathbb{C}$ (see for example [13])

$$H^-(\phi + ik) \triangleq qe^{-i(\phi+k\Delta z_0)}\mathcal{E}^-(ik)\,, \\ H^+(\phi + ik) \triangleq qe^{-i(\phi+k\Delta z_0)}\mathcal{E}^+(ik). \tag{28}$$

For the upstream case the dynamics equations become

$$\phi_0 = \phi_0^- + Im\left[K^- \frac{\partial}{\partial ik} H^-(\phi_0 + i\bar{k}^-)\right], \\ W_0 = W^- - Im\left[\frac{\partial}{\partial\phi} H^-(\phi_0 + i\bar{k}^-)\right], \tag{29}$$

where $W_0 = W(k_0)$ is the (unknown) energy at the center of the gap. For the downstream case we have

$$\phi_0^+ = \phi_0 + Im\left[K^+ \frac{\partial}{\partial ik} H^+(\phi_0 + i\bar{k}^+)\right], \\ W^+ = W_0 - Im\left[\frac{\partial}{\partial\phi} H^+(\phi_0 + i\bar{k}^+)\right], \tag{30}$$

where $W^+ = W(k^+)$. Equation (16), continuity of energy across $z = 0$, appears in this context as

$$\Delta W = Re\left[H^-(\phi_0 + i\bar{k}^-) + H^+(\phi_0 + i\bar{k}^+)\right]. \tag{31}$$

The Hamiltonian imaginary parts contain the dynamics while the real parts represent energy conservation.

SIMULATION

These techniques have been implemented in the Open XAL online model (see [14] for model, [15] for Open XAL). Each gap within a cavity contains unique spectra $\mathcal{E}^-$ and $\mathcal{E}^+$. The dynamics are computed with algorithms based on Eqs. (29), (30), (31). Compared are simulation results with the previous acceleration mechanism versus the new technique. The previous model was implemented according to the gap model described in [1]. Two situations are of primary interest, warm structures and cold structures. Results from the SNS warm linac did not demonstrate any significant differences and are not presented. More interesting findings were seen in cold structures, a comparison for the SNS medium-beta super-conducting linac is shown in Figure 1. There the initial acceleration falls off in the new model but then accelerates more strongly. The final energies are nearly equal with the new model yielding a value approximately -0.5% of the old model results. However, simulating the entire cold linac a difference of -2.4% is observed. The super-conducting gaps have more irregular fields and the new model can better represent these features.

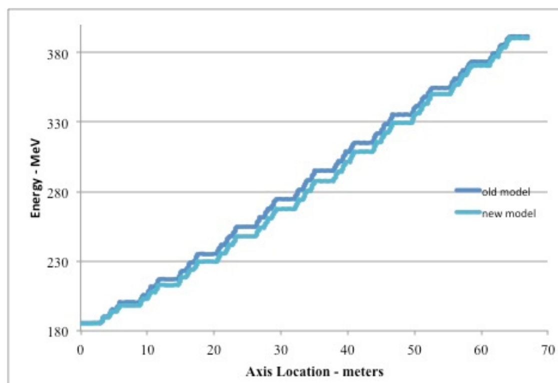

Figure 1: simulation comparison for medium-beta SCL

CONCLUSION

The current model generalizes previous treatments of the thin-lens RF accelerating gap. The full compliment of four transit-time factors allows the consideration of any axial electric field profile and is not restricted to fields symmetric about a given axis location. Moreover, the spectral analysis provided by the Laplace and Hilbert transforms is theoretically compact and more satisfying. The gap model was incorporated into the Open XAL online model. Each individual gap can be provided with unique spectra. When gap geometries are irregular or vary within a cavity the new model is useful, for example in cold accelerating structures. However, for cavities with symmetric, regular geometries the current model offers little advantage.

ACKNOWLEDGMENT

This material is based upon work supported by the U.S. Department of Energy, Office of Science, Office of Basic Energy Sciences under contract number DE-AC05-00OR22725.

Copyright © 2017 CC-BY-3.0 and by the respective authors

REFERENCES

[1] P. Lapostolle, "Proton Linear Accelerators: A Theoretical and Historical Introduction," LA-11601-MS, July, 1989, Chapt. 5.

[2] P. Lapostolle and M. Weiss, "Formulae and Procedures Useful for the Design of Linear Accelerators," CERN-PS-2000-001

[3] T. Wangler, *Principles of RF Linear Acceleration* (Wiley, New York, 1998), Sect. 2.2, 7.3.

[4] A. Shishlo and J. Holmes, "Physical Models for Particle Tracking Simulations in the RF Gap," ORNL TechNote ORNL/TM-2015/247 (June, 2016).

[5] T.L. Owens, M.B. Popovic, E.S. McCrory, C.W. Schmidt, and L.J. Allen, "Phase Scan Signature Matching for Linac Tuning," *Particle Accelerators* Vol. 48, pp. 169-179 (1994).

[6] W.R. LePage, *Complex Variables and the Laplace Transform for Engineers* (Dover, New York, 1961), Chapt. 11, p. 350, Chapt. 10, p. 285, 308, 310.

[7] E. Stein and G. Weiss, *Introduction to Fourier Analysis on Euclidean Spaces* (Princeton University Press, 1971).

[8] E.C. Titchmarsh, *Introduction to the theory of Fourier integrals* (2nd ed.), (Oxford University: Clarendon Press 1948).

[9] S. Haykin, *Communication Systems*, Third Edition (Wiley, 1994), Appendix A6.3.

[10] S. Olver, "Computing the Hilbert Transform and its Inverse," *Math. Comp.* Vol. 80 (2011), pp. 1745-1767.

[11] S.A. Tretter, *Communication System Design Using DSP Algorithms* (Springer, 2015), Chapt. 5.

[12] J. Brown and R. Churchill, *Complex Variables and Applications* (McGraw-Hill, 9 Ed., 2013), Chap. 2.

[13] V.I. Arnold, Mathematical Methods of Classical Mechanics (Springer-Verlag, 2 edition, 1989). p. 65.

[14] C.K. Allen, T.A. Pelaia, J. Freed, "Architectural Improvements and New Processing Tools for the Open XAL Online Model," IPAC2015, Richmond, Virginia, USA, May 3-8, 2015, MOPWI047.

[15] Open XAL Project Site, https://openxal.github.io and https://github.com/openxal

Copyright © 2017 CC-BY-3.0 and by the respective authors